The Pennsylvania State University

The Graduate School

Department of Meteorology and Atmospheric Science

SENSITIVITY OF SIMULATED TROPOSPHERIC OZONE IN THE MID-ATLANTIC REGION IN JUNE 2016 USING THE WRF-CHEM MODEL

A Thesis in

Meteorology

by

Andrew Michael Thomas

Submitted in Partial Fulfillment
of the Requirements
for the Degree of

Master of Science

December 2017

The thesis of Andrew Michael Thomas was reviewed and approved* by the following:

Amy K. Huff
Assistant Professor of Meteorology
Thesis Co-Advisor

Fuqing Zhang
Professor of Meteorology
Thesis Co-Advisor

William Henry Brune
Distinguished Professor of Meteorology

Johannes Verlinde
Professor of Meteorology
Associate Head, Graduate Program in Meteorology

*Signatures are on file in the Graduate School

ABSTRACT

Numerical predictions of tropospheric ozone, a secondary pollutant harmful to human health, contain large sources of uncertainty. Various studies have been conducted on the influence of meteorological initial and boundary conditions, PBL scheme, and emissions inventory, but there is no published comparative study. To address this need, we ran seven simulations of WRF-Chem, a regional online atmospheric chemistry model, with different emissions inventories, PBL parameterizations, and emissions inventories over the eastern United States within the Mid-Atlantic region. The simulations were run for June 2016, which had multiple occurrences of high mixing ratios of observed ozone within the Mid-Atlantic region, particularly along the urbanized Interstate-95 Corridor. Special attention was paid to the 20% of days with the highest observed ozone. Our analysis of the average standard deviation of 8-hour average ozone showed that ground-level ozone was most sensitive to the uncertainty in the initial and boundary conditions, with peaks in average standard deviation of 6 to 7 ppbv, while the emissions inventory uncertainty was of secondary importance with peaks in the average standard deviation of 4 to 5 ppbv. We compared the temporal average of the ensemble members and showed that the emissions inventory has the greatest influence on the average ozone mixing ratio. The ERA-interim generated more ozone than the other initial and boundary conditions ensembles, with ground-level peaks of 70 to 75 ppbv 8-hour averaged ozone. In comparison to the emissions inventory and the meteorological initial and boundary conditions, tropospheric ozone was less sensitive to the PBL scheme. The modeled sensitivity was enhanced aloft over Interstate 95, a source of ozone precursor emissions from mobile sources. Based on our data, we estimated that updating the emissions inventory yields an average decrease of 0.6 ppbv yr^{-1} in the mean absolute error, and an average decrease of 0.8 ppbv yr^{-1} in mean daily eight-hour ozone. There are many

avenues for further research, including expanding the ensemble size. Our results suggest that the choice of initial and boundary conditions may affect other air quality studies.

TABLE OF CONTENTS

LIST OF FIGURES

LIST OF TABLES

ACKNOWLEDGEMENTS

Firstly, I would like to thank my advisers. I thank Amy for her patience, especially during the early stages of my research. I would like to thank Fuqing, for without his unyielding confidence in me, I would not have gotten the opportunity to conduct research. I would also like to thank many contributors, including those who have reviewed this paper, my committee member Dr. Brune, Dr. Xiaoming Hu, who helped me learn how to use WRF-Chem, and Dr. Daniel Tong, who provided the data required to create the NEI-14. I would like to thank all the friends I have met here at PSU, through the Department of Meteorology, through Disciplemakers Christian Fellowship, and through St. Paul's UMC/Wesley Foundation- you made my time here much more enjoyable. I also want to thank my family, for putting up with my months of radio silence and struggles through the years.

Chapter 1

Introduction

Tropospheric ozone, one of the U.S. Environmental Protection Agency (EPA)'s seven criteria pollutants, has been linked to a litany of health problems, including cardiovascular disease (Azevedo et al. 2011), infant mortality (Bell et al. 2004), and asthma (Gent et al. 2003). To mitigate these health risks, air quality forecasts of ozone are regularly made with the assistance of Eulerian air quality models. Since the accuracy of air quality forecasts is a matter of national health, especially for sensitive groups as defined by the National Ambient Air Quality Standards (NAAQS), air quality forecasters should know the current sources of uncertainty within the numerical guidance.

Eulerian air quality modeling is a multifaceted problem that depends on economic forcing (Tong et al. 2016), meteorological conditions (Seaman 2000), and chemistry. Each of these processes have a practical predictability, which is the uncertainty given current methods, that is contrasted against intrinsic predictability—the limit of the uncertainty of a perfectly modeled system (Melhauser and Zhang 2012; Lorenz 1969; Zhang et al. 2006). For this study, we will only study uncertainty as it pertains to practical predictability, since we want to target research areas to maximize the accurate prediction of tropospheric ozone, in preparation for operational usage of the Weather Research and Forecasting Model with Chemistry (WRF-Chem; Grell et al. 2005). We chose WRF-Chem, because it computes chemistry alongside the meteorology, rather than the Community Multiscale Air Quality Model (CMAQ; Byun et al. 1997), which treats atmospheric chemistry as a postprocess. The advantages of computing chemistry alongside the

meteorology, as explained within Grell et al. (2005), were related to the loss of information between time steps of model output, at the cost of additional computations.

The model uncertainty of tropospheric O_3 is influenced by several settings. The most notable settings that contribute to the uncertainty of tropospheric O_3 are the physical parameterizations, initial and boundary conditions, and anthropogenic emissions inventory (Mallet and Sportisse 2006; Cuchiara et al. 2014; Misenis and Zhang 2010; Mena-Carrasco et al. 2009). Physical parameterizations, equations that approximately emulate sub-grid phenomena, are methods representative of the current understanding of the physical process. The variety of solutions of the parameterizations is representative of the diverse understanding of those processes and is one aspect of practical predictability of tropospheric O_3. Varying initial and boundary conditions are within the definition of practical predictability, for it is not reasonable to know the true state of the atmosphere, differentiating practical predictability from the intrinsic predictability (Melhauser and Zhang 2012). The definition of practical predictability also contains the anthropogenic emissions inventory, as real-time point and area emissions are not available presently.

Several studies have been done on the sensitivity of ozone to physical parameterizations. Mallet and Sportisse (2006) indicated that ozone is most sensitive to the uncertainty in the turbulence closure, which is embodied in the Planetary Boundary Layer (PBL) scheme within WRF-Chem. Some studies indicate that the Yonsei University (YSU) PBL scheme shows the closest agreement between predicted ozone and observed ozone (Yerramilli et al. 2010; Cuchiara et al. 2014; Cheng et al. 2012). Although Yerramilli et al. (2010) claims that ozone is more sensitive to uncertainty in the Land Surface Model (LSM), Pleim (2011) notes that there are deficiencies in that study, including the fact that the second version of the Asymmetric Convective Model (ACM2) at that time was not implemented for use with tracers within WRF-Chem. Since then other studies, such as Cuchiara et al. (2014), have used ACM2 within WRF-

Chem, since diffusion in WRF-Chem was implemented in 2013. Some other studies, such as Misenis and Zhang (2010), corroborate the claim that ozone may be more sensitive to uncertainty in the LSM than the PBL scheme, though Hodnebrog et al. (2011) suggested that the sensitivity of ozone to uncertainty in the LSM may be confined to certain regions.

While the variety of choices of the PBL scheme represents the large uncertainty of a solitary meteorological process, emissions inventory uncertainty, which represents the uncertainty of anthropogenic emissions within the United States, is also large. O_3 is formed from the reaction of atomic oxygen with molecular oxygen following a set of reactions involving O_3 precursors, which include nitric oxide (NO), nitrogen dioxide (NO_2) and volatile organic compounds. Within the United States, anthropogenic NO and NO_2, collectively named NO_x, has been decreasing since at least 2005 (Tong et al. 2015). Tong et al. (2015) also shows that NO_x emissions have been decreasing, but still retain both temporal and spatial variability. Uncertainty in emissions inventories occur due to changes in emissions control devices, activity, and changes in emission factors, among other reasons. Of the emission inventories available to users of WRF-Chem, the gridded version of the National Emissions Inventory (NEI) series from the U.S. Environmental Protection Agency (EPA) has the highest spatial resolution and includes buoyant plume rise, making the NEI emissions inventories ideal for simulations within the continental United States, since higher resolution emissions inventories are important for local air quality studies (Hodnebrog et al. 2011). The NEI gridded emissions inventories are updated approximately every six years, with the latest emissions inventory being representative of a typical July weekday in 2011 (NEI-11). The point sources are compiled by the EPA, according to the Air Emissions Reporting Rule. The mobile emissions sources were processed using the Motor Vehicle Emissions Simulator (MOVES), which Anderson et al. (2014) claimed had the most uncertainty. For more information on the construction of the NEI-11, please see EPA (2015).

Since accurate NO_x prediction is a condition for accurate predictions of O_3, and the anthropogenic emissions inventories contain large uncertainties, errors in NO_x may lead to errors in O_3. Travis et al. (2016) showed that the NEI-11 may be overestimating emissions up to a factor of 2, demonstrating that the overestimation of NO_x emissions leads to overestimation of O_3 in NO_x-limited environments. While Travis et al. (2016) agrees with Anderson et al. (2014), the recommended decrease in NO_x varies, indicating that there is uncertainty with the precise decrease needed. The National Air Quality Forecasting Capability (NAQFC; Davidson et al. 2008, Otte et al. 2005) model, an operational CMAQ model, adjusted the NO_x emissions for 2012 and found that the NO_x bias decreased between 0.57 and 2.34 ppbv, while the decrease in ozone bias was between 0.92 and 1.87 ppbv (Pan et al. 2014). Other studies in different areas yielded varying results. Zhong et al. (2016) provide one example of the sensitivity of O_3 in China due to discrepancies between one regional and one global emissions inventory, with differences between 12-16 ppbv of O_3 in certain locations, showing that the sensitivity of O_3 to emissions inventory is location-specific. Going further than simply comparing emissions inventories, some studies have examined the response of ozone due to certain sources (Vijayaraghavan et al. 2012), and temporal variability (Castellanos et al. 2009) of emissions sources.

While the emissions inventory is a major source of uncertainty, the initial and boundary conditions are critical for determining the evolution of the model. Lorenz (1963) demonstrated the influence of perturbations of the initial state on the evolution of nonperiodic flow; the initial conditions of the atmosphere determine its future state; this includes the composition. While chemical initial and boundary conditions are important (Berge et al. 2001), the influence of chemical initial conditions can be constrained with a spin-up time of 48 hours, to reduce the correlation on initial conditions by 10% (Jiménez et al. 2007). Bei et al. (2010) suggests that meteorological initial conditions contribute more uncertainty to O_3 mixing ratios in Mexico City, with the ensemble spread reaching 15 ppbv over Houston. Zhang et al. (2007) noted that, for a

high O_3 event in Houston, Texas, the spread of ensemble members with different initial (and boundary) conditions peaked with 40 ppbv of hourly O_3 values over the Gulf of Mexico and 20 ppbv over one of the Texas stations. Gilliam et al. (2015) also observed a spread as high as 10-20 ppbv over the Northeastern United States, while using the Short-Range Ensemble Forecasting system members as initial and boundary conditions. However, Beekmann and Derognat (2003) suggest that the O_3 sensitivities may range from 4-10 ppbv over Paris. Discrepancies in the ranges of sensitivities may be a result of a variety of reasons, including the methods of perturbations of initial and boundary conditions, the quantity of O_3 precursors emitted, the effect of local topography, and the meteorological variability.

Many of the referenced studies focus on different days in different locations with NAAQS-exceeding mixing ratios of the Maximum Daily 8-Hour Running Average mixing ratio of O_3 (MD8-O_3), so the studies may be incomparable. We investigated and compared the relative impacts of the uncertainty in the emissions inventory, the PBL scheme, and the initial and boundary conditions on MD8-O_3 by running several WRF-Chem simulations over the eastern United States for June 2016. While the simulations were conducted over the eastern United States, special attention was given to the I-95 corridor, so that the uncertainty of MD8-O_3 was quantified to improve air quality forecasts to areas plagued by NAAQS-exceeding MD8-O_3 within the Mid-Atlantic region. Those simulations included the YSU, Mellor-Yamada-Janjic scheme (MYJ), and ACM2 PBL schemes, the NEI-11, NEI-05, NEI-14 emissions inventories, and GFS, European Center for Medium Range Weather Forecasting interim Reanalysis (ERA-interim), and the second version of the Modern Era Retrospective analysis for Research and Applications (MERRA-2) meteorological initial and boundary conditions.

Chapter 2

Methods

The Upper-Quintile and Climatology of Ozone in the Mid-Atlantic Region

In June 2016, multiple stations observed NAAQS exceedances of MD8-O_3 over several days within the Northeast Megalopolis and the surrounding area. Furthermore, the Philadelphia, Baltimore, and Washington D.C. metropolitan areas observed Moderate (Code Yellow on the Air Quality Index scale) mixing ratios of MD8-O_3 for 17, 13, and 14 days, respectively. Given the plethora of days with Moderate or above MD8-O_3, the 20% of days with the highest observed MD8-O_3, hereafter called the upper-quintile, were chosen to be focused on. Those dates were chosen based on the number of stations in eastern Pennsylvania, New Jersey, Maryland, and Delaware that were in nonattainment of the NAAQS. The seven dates that satisfy those criteria were June 1st, 11th, 15th, 20th, 24th, and 26th, which had 20, 15, 4, 20, 8, and 2 stations that measured MD8-O_3 mixing ratios over 70 ppbv. Figure 1: MD8-O_3 of the constituent days of the upper-quintile. details the observed MD8-O_3 for each date in the upper-quintile.

Climatologically, high mixing ratios of O_3 within the Mid-Atlantic region are caused by the western extent of the semi-permanent Bermuda High, a synoptic scale high pressure ridge leading to the stagnation of surface winds, long-range transport from the Ohio River Valley, and subsidence that reduces cloud coverage (Ryan et al. 1998). Considering that the synoptic scale ridge reduces cloud coverage, photolysis of ozone and the enhancement of the emissions of biogenic emissions are maximized, leading to heightened MD8-O_3. Since the baseline O_3 mixing ratio has decreased in the Mid-Atlantic region in the past several years due to NO_x emission decreases, the climatology of O_3 is no longer consistently reliable due to the elimination of the stationarity assumption (Ryan 2016). During June 2016, the synoptic scale ridge was still a

pattern associated with NAAQS exceeding MD8-O_3 during the upper-quintile days. June 1st and 20th observed similar weather patterns as those described by Ryan et al. 1998 and observed the most NAAQS exceeding MD8-O_3 monitors. On the other upper-quintile days, which were the 11th, 15th, 24th, and 26th, O_3 formation was enhanced by mesoscale features which increased flux convergence and transport of O_3 and O_3 precursors. An example of the enhancement of O_3 by a sea breeze circulation in the Mid-Atlantic region was given in Stauffer et al. (2015). Another example is shown in Seaman and Michelson (1998), which examined the influence of a lee trough on enhancement of O_3.

WRF-Chem Simulations

A control simulation, designated CNTL, of WRF-Chem version 3.6.1, was run for June 2016, with a two-day spin-up period in May. The meteorological initial and boundary conditions were reinitialized every two days at 12 UTC by the Global Forecasting System (GFS) from the NOAA Operational Model Archive and Distribution System (NOMADS), with the missing GFS NOMADS data of June 23rd replaced by GFS data from the National Center for Environmental Prediction. The chemical fields were kept continuous. The PBL scheme used by the CNTL simulation was the Yonsei University (YSU; Hong et al. 2006) scheme. The CNTL simulation uses the NEI-11 emissions inventory. In addition to the model settings described by Table 1, all the simulations had a domain spanning from the Mississippi River to southern Maine with 12 kilometer (km) horizontal resolution, as is depicted in Figure 2. The vertical model structure is the same as described by Hu et al. (2012). In Figure 2, major cities are marked and labeled in the Analysis Region. The Analysis Region contains much of the Northeast Megalopolis, and I-95, which is marked in red. We made the WRF-Chem domain more expansive than the Analysis Region to account for anthropogenic sources of NO_x upwind of the WRF-Chem domain.

The CNTL simulation was repeated six times to form an ensemble. Each ensemble member had either the PBL scheme, emissions inventory or the meteorological initial and boundary conditions changed. The grouping of alterations is denoted as a sub-ensemble, such that all members of the sub-ensemble, hereafter called sub-ensemble members, have one specific feature altered. The names of each member and the denoted group is detailed by Table 2. The emissions sub-ensemble consisted of a simulation using the 2005 version of the National Emission Inventory (NEI-05) and a version of the NEI-11 updated to reflect emissions of nitrogen monoxide (NO) in 2014 (NEI-14). The weekday emissions of the NEI-05 were used, since only the weekday emissions of the NEI-11 were available. The NO point emissions of the NEI-14 were updated for each hour by using the average of the Clean Air Market data. The area emissions were updated for each state by using statewide ratios of NO_x emissions in 2014 to NO_x emissions within the NEI-11, which were contributed by NOAA (personal communication). The creation of the NEI-14 loosely follows the methodology used to update the North American Air Quality Forecast Capability (NAQFC) model.

The next sub-ensemble consists of repeating the CNTL simulation with different PBL schemes. The CNTL uses the YSU scheme, which is a non-local parabolic K-scheme that defines entrainment. The other two members consist of the second version of the Asymmetric Convective Model (ACM2) and the Mellor-Yamada-Janjic (MYJ) scheme. The ACM2 is a hybrid local/nonlocal PBL scheme, which treats upward mixing nonlocally and downward mixing locally. In contrast to the YSU scheme used by the CNTL simulation, the MYJ scheme is a local K-scheme. As noted in Skamarock et al. (2005), the WRF model constrains some PBL schemes to certain surface layer physics. Therefore, the member that utilized the MYJ PBL scheme used the Eta similarity surface layer physics (Monin and Obukhov 1954), while the ACM2 and YSU PBL schemes use the Revised MM5 surface layer physics (Jiménez et al., 2012).

The last sub-ensemble contained differing initial and boundary conditions from different models. One sub-ensemble member used the second version of the Modern Era Retrospective reanalysis (MERRA-2) from the National Aeronautics and Space Administration. MERRA-2 is a reanalysis dataset that utilizes the Goddard Earth Observing System model with a 3D-Variational data assimilation system. The approximate resolution of MERRA-2 is 0.5° x 0.625° with 72 vertical levels (Gelaro et al., 2017). The other source of the initial and boundary conditions is the ERA-interim reanalysis from the European Centre for Medium-Range Weather Forecasts (ECMWF). The ERA-interim reanalysis uses the ECMWF model with T255 resolution (approximately 80 km) with a 4D-Variational data assimilation system (Dee, 2011). The soil temperature, moisture, and depth for all simulations were taken from the GFS, such that only meteorological data was varied among sub-ensemble members. All inputted datasets were temporally interpolated, to the extent that the boundary conditions were updated hourly.

Although the domain ranges from the Mississippi River to southern Maine, special interest was paid to the northern Mid-Atlantic Region. In this region, denoted the Analysis Region, nonattainment of the 2010 NAAQS for MD8-O_3 spans over eastern Pennsylvania, New Jersey, Delaware, and Maryland. In this Analysis Region, we calculated the sensitivity of MD8-O_3, expressed by the standard deviation of each sub-ensemble of the upper-quintile. We also examined the vertical distribution of MD8-O_3, and sensitivity thereof, along the model-interpolated United States Interstate 95 and the New Jersey Turnpike (I-95), which passes through the Northeastern Megalopolis. Additionally, we evaluated the effect of the changing emissions inventory on predicted MD8-O_3.

Chapter 3

Results and Discussion

Average Ensemble Differences

Figure 3 shows the temporal average of surface level MD8-O_3 during the upper-quintile for each ensemble member in the Analysis Region, as compared to the similarly processed observations. The model-interpolated location of I-95 is marked in white. Each ensemble member overproduced MD8-O_3 in the Analysis Region, but the NEI-05 ensemble member produced the most ozone among the ensemble. The ERA ensemble member also showed overproduction of ozone, but the overprediction of the ERA has a smaller maximum as compared to the overprediction of the NEI-05. The cause of the overprediction of the ERA member was not well understood, though one hypothesis suggested that the ERA promoted vertical transport of O_3 and O_3 precursors from the residual layer. In addition to the information about the emissions inventories and the initial and boundary conditions, Figure 3 also displays few differences in MD8-O_3 due to PBL scheme. Among the PBL sub-ensemble for the upper-quintile, there was no definitively accurate scheme, as compared to the other settings tested. This result neither validated nor invalidated the work of Yerramilli et al. (2010), Cuchiara et al. (2014), or Cheng et al. (2012), but emphasized that the choice in PBL scheme was less significant for differences of the average MD8-O_3 than the initial and boundary conditions and emissions inventory.

Comparing the model predictions to the observations, Figure 3 implies overprediction of MD8-O_3. However, the overproduction of MD8-O_3 was not quantified in Figure 3, but in Figure 4. Figure 4 showed the mean bias of each ensemble member during the upper-quintile. The NEI-05 overpredicted MD8-O_3 more than any other ensemble member, which is shown by the monitors which the NEI-05 overpredicted MD8-O_3 by 30 to 35 ppbv in northern North Carolina

and Virginia. In contrast, the NEI-14 overpredicted less MD8-O_3 than the other emissions inventory sub-ensemble members, as illustrated by the exaggeration in the underpredicted region of New Jersey and the New York metropolitan area. The reduced overproduction of the NEI-14 indicates that updated emissions will lead to more accurate predictions of MD8-O_3. The ERA ensemble member overproduced ozone more than any other initial and boundary condition sub-ensemble member, illustrated by the few monitors that underpredicted O_3 in New Jersey and New York city metropolitan area. The MERRA-2 sub-ensemble member overpredicts the least amount of ozone of any ensemble member, but only by less than 0.5 ppbv than the NEI-14. All ensemble members showed average overprediction of MD8-O_3 in the southern portion of the Analysis Region. The average overprediction of MD8-O_3 in the southern part of the Analysis Region was partially explained by the average overestimation of NO_x within the emissions inventories (Travis et al. 2016) and biogenic emissions (Fiore et al. 2005, Bell and Ellis 2004). While MD8-O_3 is overpredicted on average, New Jersey and the New York Metropolitan area has areas of underpredicted MD8-O_3. Since the updated emissions inventory underpredicted more than older emissions inventories, updating the emissions inventory was not a cause for this underprediction. However, the magnitude and spatial extent of the underprediction changes with different initial and boundary conditions, with the underprediction of the ERA member being less than the CNTL or MERRA-2 members. Since our hypothesis is that the ERA member produced more MD8-O_3 due to convective vertical transport, then the underprediction of vertical transport may be explained by compensated by inaccurate modeling of convection.

The temporal average during the upper-quintile of the cross-sectional MD8-O_3 over I-95 is displayed in Figure 5. The magenta dashed line represents the upper-quintile averaged peak eight-hour averaged PBL height. The latitudes of major cities are marked and labeled by dashed lines. The vertical coordinate was computed using the hypsometric equation of the upper-quintile averaged hydrostatic pressure and temperature during the same period that the surface MD8-O_3

was modeled. In the southern part of I-95, MD8-O_3 was produced more by the NEI-05 than any other member. The peak values of MD8-O_3 were not in the urban areas, but outside the urban areas. The overproduction of MD8-O_3 due to the NEI-05 in the southern Analysis Region was most prominent between one and two kilometers aloft, near the height of the boundary layer, where the average mixing ratio reached over 85 ppbv. The only other ensemble member to have exceeded 85 ppbv aloft was the MYJ, but the NEI-05 produced a larger area of MD8-O_3 aloft that exceeded 85 ppbv. Since O_3 is transported further distances aloft, this implies that the emissions inventory was more influential in the magnitude of the long-range transport of O_3 than the PBL scheme. Additionally, the ERA member showed that the overproduced ozone was enhanced aloft by 5 ppbv as compared to both the MERRA-2 and CNTL simulations. The overprediction of the ERA member is consistent with the hypothesis that the ERA member promotes convection, leading to enhancement of MD8-O_3.

Sensitivity of MD8-O_3

While we have discussed the variability and patterns of the upper-quintile average MD8-O_3, we have yet to discuss the upper-quintile average *of the variability* of MD8-O_3. Figure 6 displayed the upper-quintile average standard deviation of near-surface MD8-O_3 for each sub-ensemble. The model-interpolated location of I-95 is denoted by the white line. This figure illustrates that initial and boundary conditions had a larger variability than both the emissions inventory and PBL scheme sub-ensembles. The initial and boundary conditions had a peak sensitivity of 6 to 7 ppbv, which is contrasted against the peak sensitivities of 4 to 5 ppbv due to changes in the emissions inventory and PBL scheme. This implies that the sensitivity of MD8-O_3 for the upper-quintile was influenced more by the meteorological conditions on those days than the emissions inventory. After the initial and boundary conditions, the variation in emissions

inventory was a secondary source of uncertainty for MD8-O_3, despite having similar peaks in sensitivity. The average sensitivity of MD8-O_3 due to the emissions inventory covered a larger area than the sensitivity of MD8-O_3 due to uncertainties in the PBL scheme. Although the uncertainty of MD8-O_3 may be largest for the initial and boundary conditions, that does not necessarily indicate that the uncertainty was largest at every point. For example, MD8-O_3 in southern New Jersey was more sensitive to uncertainty in the emissions inventory than uncertainty in the initial and boundary conditions by approximately 1 ppbv. Additionally, the largest uncertainties of the initial and boundary conditions may not be collocated with the highest values of MD8-O_3. For example, I-95, which connects major cities in the Analysis Region, runs along the outside edge of the large uncertainty.

Over I-95, the upper-quintile averaged sensitivity of MD8-O_3 was largest due to initial and boundary conditions, as illustrated by

Figure 7. The dashed magenta line denotes the sub-ensemble averaged and temporally averaged PBL height. While the MD8-O_3 aloft was most sensitive to uncertainty in the initial and boundary conditions, the sensitivity due to uncertainty in the emissions inventory was larger aloft over the southern part of the Analysis Region. This agrees with Travis et al. (2016) that the emissions inventory represents a large source of error for the southeastern United States. Also, the most uncertainty associated with the emissions and initial and boundary conditions sub-

ensembles was located near the top of the boundary layer. This increase in the sensitivity of ozone with height is consistent with the hypothesis that the ERA promotes convective vertical transport of O_3 and O_3-precursors.

While Figure 6 showed how the uncertainty of MD8-O_3 was distributed in space, Figure 8 showed which days have the most uncertainty of MD8-O_3, by displaying the spatially-averaged standard deviation of each sub-ensemble, not including areas over bodies of water. The constituent days of the upper-quintile are marked by solid black lines, except for June 1st, which overlaps with the x-axis. The initial and boundary conditions sub-ensemble frequently had the most uncertainty. However, the average standard deviation of the sub-ensemble was smaller than the mean absolute error of the ensemble members, as given in Table 3 and Figure 9. This indicates that all the sub-ensembles were under-dispersive, even without chemical data assimilation. This result also shows a smaller standard deviation than the findings of Gilliam et al. (2015), but this may be due to using three members used by the initial and boundary conditions sub-ensemble. By comparison, Gilliam et al. (2015) used ten SREF-initialized WRF-CMAQ simulations, as compared to our three multi-model initialized WRF-Chem simulations. Our results for the initial and boundary conditions uncertainty over land were of similar order to those presented in the "half-run" in Zhang et al. (2007). The similarity of the initial and boundary conditions sub-ensemble uncertainty to the "half-run" uncertainty of Zhang et al. (2007) implies that the initial differences between the CNTL, ERA, and MERRA-2 simulations were representative of about half the variability of the initial ensemble employed by Zhang et al. (2007).

Although the initial and boundary conditions have the most uncertainty of the sub-ensembles, the initial and boundary condition sub-ensemble was under-dispersive, which occurs when the error is smaller than the ensemble uncertainty. Consider Figure 10, which shows the timeseries of MD8-O_3 of the emissions and initial and boundary conditions sub-ensembles at The

Rutgers University station, which is representative of the New York Metropolitan area. The Rutgers University station observed four days with NAAQS exceedances of MD8-O_3. Of those four days, three days occurred during the upper-quintile. Of the 30 observations of MD8-O_3 taken at the Rutgers University station, 23 observations were outside the range of solutions of the initial and boundary conditions sub-ensemble, and 25 observations were outside the range of solutions of the emissions inventory sub-ensemble. Since 23 of the 30 observations were outside the sub-ensemble ranges, both sub-ensembles are under-dispersive. Although the initial and boundary conditions sub-ensemble was under-dispersive, this does not imply that the initial and boundary conditions were insufficient for uncertainty estimation of ozone (such as for applications to data assimilation) since the sub-ensemble consisted of three sub-ensemble members and did not include assimilation of chemical observations. Additionally, Figure 10 supports the idea that older emissions inventories produce more MD8-O_3, enhancing the positive bias.

Emissions Inventory Analysis

Since predicted MD8-O_3 has a clear positive bias among all ensemble members, as seen in Figure 4, and the newer emissions inventories decrease error, as shown in Table 3, we estimated the average decrease of the mean absolute error due to emissions inventory updates. Figure 11 illustrates the average change of the mean absolute error of MD8-O_3 per emissions inventory year for the upper-quintile by calculating the slope of the trendline of mean absolute error over the various emissions inventory years. There was one stipulation: since only the emissions of nitric oxides were updated in the NEI-14, the changes in volatile organic compounds may alter the finding. While an average decrease of 0.6 ppbv yr^{-1} of the mean absolute error of MD8-O_3 was estimated, areas in the New York Metropolitan area indicate increases in error. The largest decreases in mean absolute error was found in Maryland, where decrease over 1 ppbv

yr^{-1} were estimated. Except for those few stations with increases, the result was logical—the updated emissions inventory was more representative of the actual emissions.

Using a similar methodology as was used to estimate the average decrease of the mean absolute error, the average decrease of MD8-O_3 during the upper-quintile was found. Figure 12 illustrates the decrease in MD8-O_3. The Analysis Region had decreasing MD8-O_3 with each emissions inventory year. Over land, the average decrease of MD8-O_3 was 0.8 ppbv yr^{-1}. The average change in the mean absolute error of MD8-O_3, as seen in Figure 11, has more positive areas than the average change of MD8-O_3. For those areas with increasing error but decreasing MD8-O_3, this implies that the changes in the emissions inventories are not representative of the actual emissions. Using the yearly averaged regional surface ozone observations for the same number of years as covered by the emissions inventory, we computed decreases of 1.67 ppbv yr^{-1}. Since the observed decrease of ozone include inter-annual variability, months other than June, and a larger space, and observational sampling. These differences may be compounding factors for the difference in modeled decreases and observed decreases.

Limitations

One important limitation of this study was the number of ensemble members. As with most research involving ensembles, the number of members used are limited by computational resources. Since WRF-Chem was computationally more expensive than simply running WRF, and we ran WRF-Chem for a month, we limited the number of ensemble members allowed within our model. Additionally, we wanted to compare the same number of ensemble members, and we had three emissions inventories available, we were limited by our choice to test the sensitivity of tropospheric ozone to uncertainty in the emissions inventory. This limitation may be one reason the uncertainty of all sub-ensembles was less than the error of the observations.

Another limitation, though less significant in breadth, was the restriction of the NEI-14 emissions inventory to only changes in NO_x. By limiting the changes in emissions within the NEI-14 to only NO_x, changes in anthropogenic emissions of VOCs were neglected and may alter the oxidative capacity. Supplemental information of NO_x emissions was more readily available than information on VOC emissions. For our analysis, we neglected the changes in VOCs on the rationale that most of the Mid-Atlantic region was in a NO_x-limited regime.

Chapter 4

Conclusions

Implications

Our results demonstrate that the tropospheric ozone was more sensitive to uncertainty in the meteorological initial and boundary conditions. This sensitivity emphasized the need for accurate data assimilation of meteorological data for accurate modeling of tropospheric ozone. In addition, our results demonstrate how the choice of initial and boundary conditions may result in systematic biases for tropospheric ozone. Therefore, the choice of initial and boundary conditions may influence the findings of other research.

Another implication of our results is the widespread sensitivity of tropospheric ozone to initial and boundary conditions and emissions inventory. While ozone is primarily a pollutant in suburban areas, the areas where the MD8-O_3 sensitivity to emissions inventories was between 3 and 5 ppbv spanned from the Blue Ridge Mountains of Virginia to central New Jersey. The breadth of sensitivity indicates that changes in emissions may also influence ozone in rural areas.

Opportunities for further research

As stated previously, one limitation in this paper was the limitation of having only three sub-ensemble members. This may be remedied by repeating the experiment with combinations of changing emissions inventories, PBL schemes, and meteorological initial and boundary conditions. Using only the three choices presented in this paper, twenty-seven different ensemble members may be created by using the emissions inventories, PBL schemes, and initial and boundary conditions. In addition to assuaging the concerns over ensemble size, the change in

sensitivity due to other parameterizations may also be investigated. With multiple configurations of the ensemble, an optimal configuration may be found. The hypothetical twenty-seven-member ensemble may be expanded upon by varying parameterizations not considered in this paper.

Furthermore, our results show a correspondence of emissions inventory age to mean absolute error. While newer emissions inventories lead to more accurate results than older emissions inventories with an improvement of 0.6 ppbv yr^{-1}, emissions inventories are updated infrequently. Therefore, updates in emissions modeling, or inverse modeling algorithms to remedy incorrect emissions, may improve accuracy.

In addition to our work, further research may be done on the underlying reason the tropospheric ozone is more sensitive to uncertainty in the initial and boundary conditions rather than uncertainty in the emissions inventory or uncertainty in the PBL scheme. Such work would investigate differences in ozone tendencies, including, but not limited to differences in the photolysis rate, chemical tendency, horizontal transport, and photostationary ozone. Similar methods may be applied to trace chemicals beyond ozone, such as ozone precursors or the various volatile organic compounds within the chemical mechanism.

Chapter 5

Figures and Tables

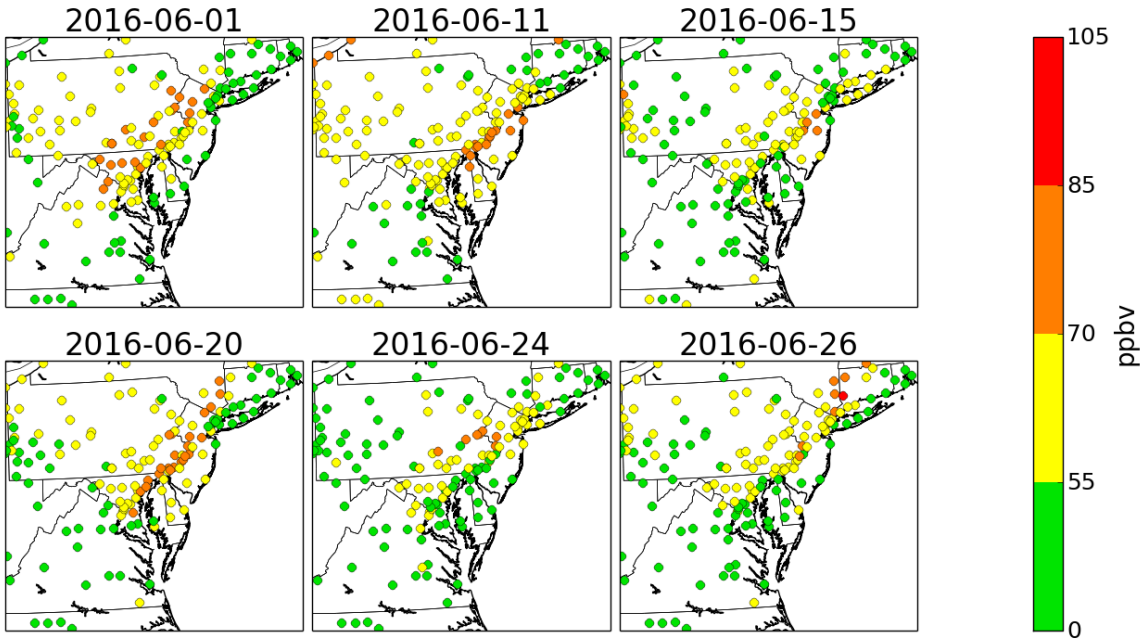

Figure 1: MD8-O_3 of the constituent days of the upper-quintile.

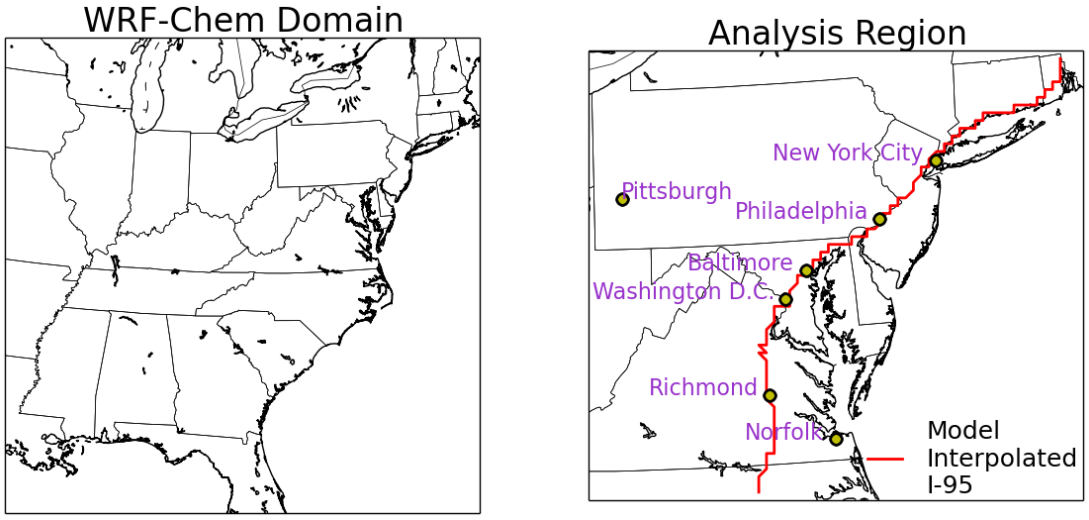

Figure 2: The simulated WRF-Chem domain (left) and the Analysis Region (right).

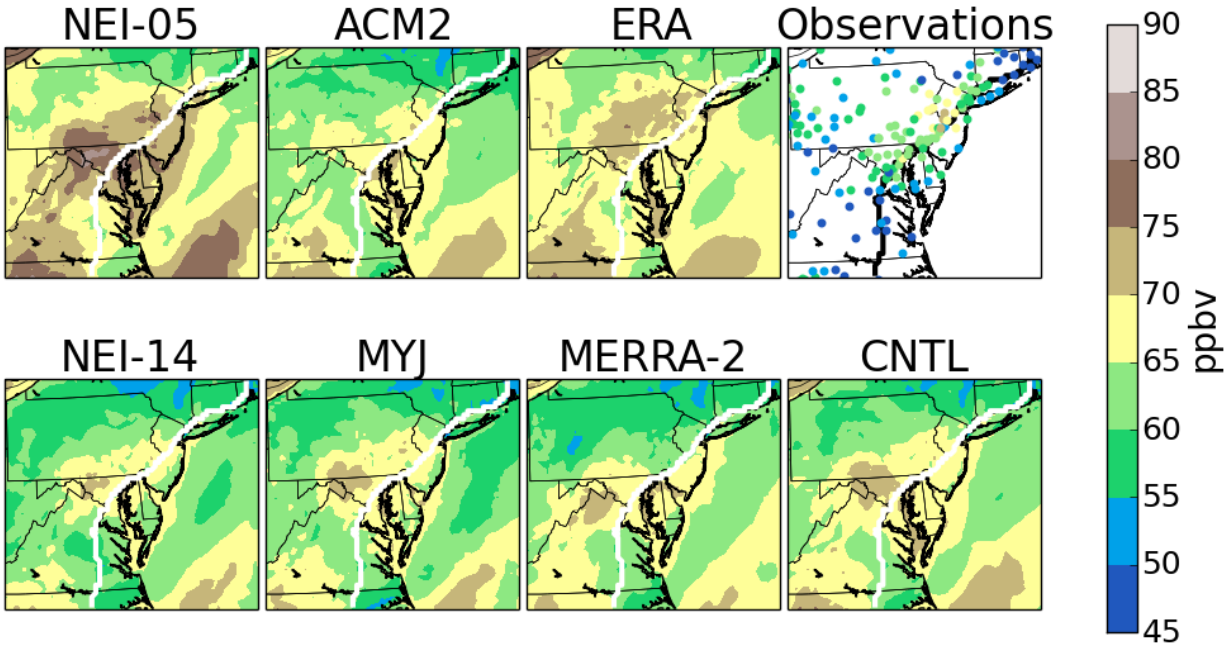

Figure 3: Temporal average of MD8-O_3 during the upper-quintile.

Table 1: CNTL model settings.

Setting	Choice	Reference
Longwave Radiation	RRTM	Mlawyer et al. 1997
Shortwave Radiation	Dudhia	Dudhia 1989
Cumulus	Grell-Devenyi	Grell and Devenyi 2002
Microphysics	WSM6	Lim and Hong 2010
Land Surface Model	NOAH	Tewari et al. 2004
Chemistry	RACM	Stockwell et al. 1997
Biogenic Emissions	MEGAN	Guenther et al. 2006
Photolysis	Madronich	Madronich 1987

Table 2: Ensemble member names and changed model settings.

Ensemble Member	PBL	IC/BC	Emissions
CNTL	YSU	GFS	2011
ACM2	ACM2	GFS	2011
MYJ	MYJ	GFS	2011
NEI-05	YSU	GFS	2005
NEI-14	YSU	GFS	2014
MERRA-2	YSU	MERRA-2	2011
ERA	YSU	ERA-GFS	2011

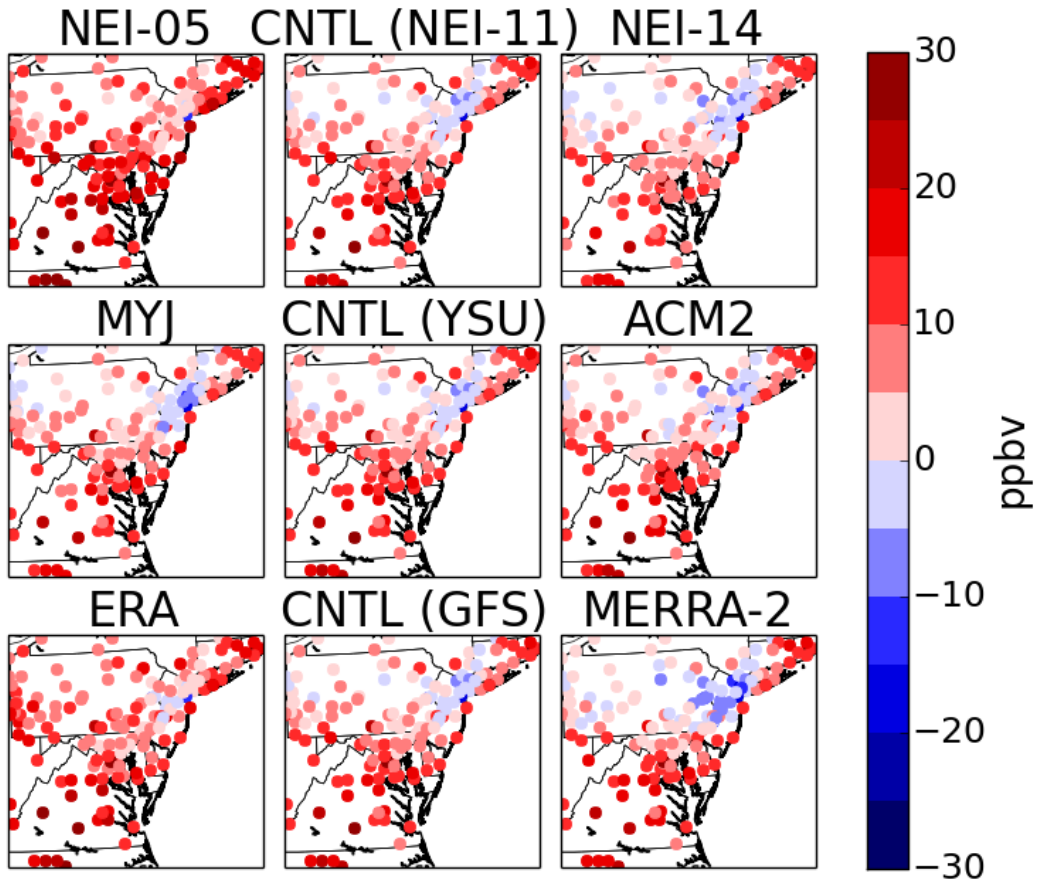

Figure 4: Mean bias of MD8-O_3 for the upper-quintile.

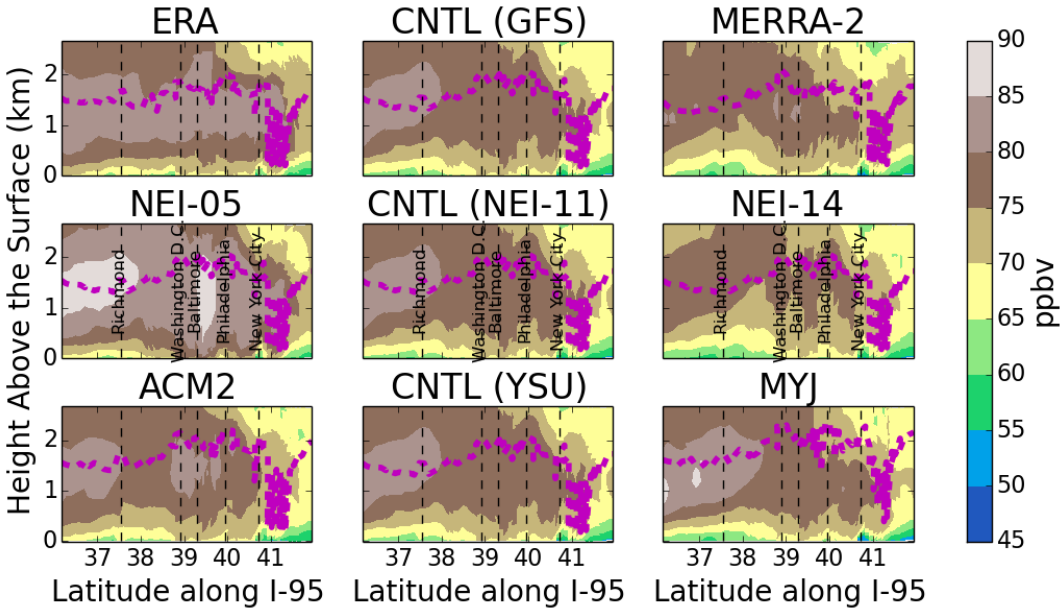

Figure 5: Average cross-section of MD8-O_3 along I-95 during the upper-quintile.

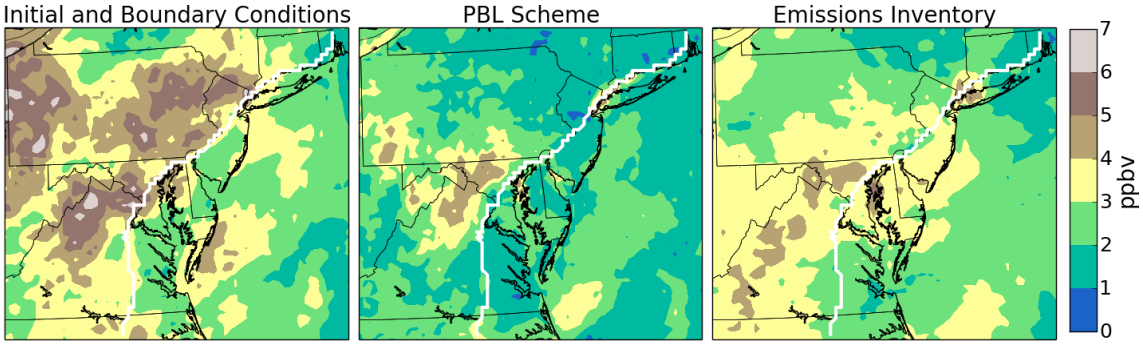

Figure 6: Temporal average of the standard deviation of MD8-O_3 during the upper-quintile.

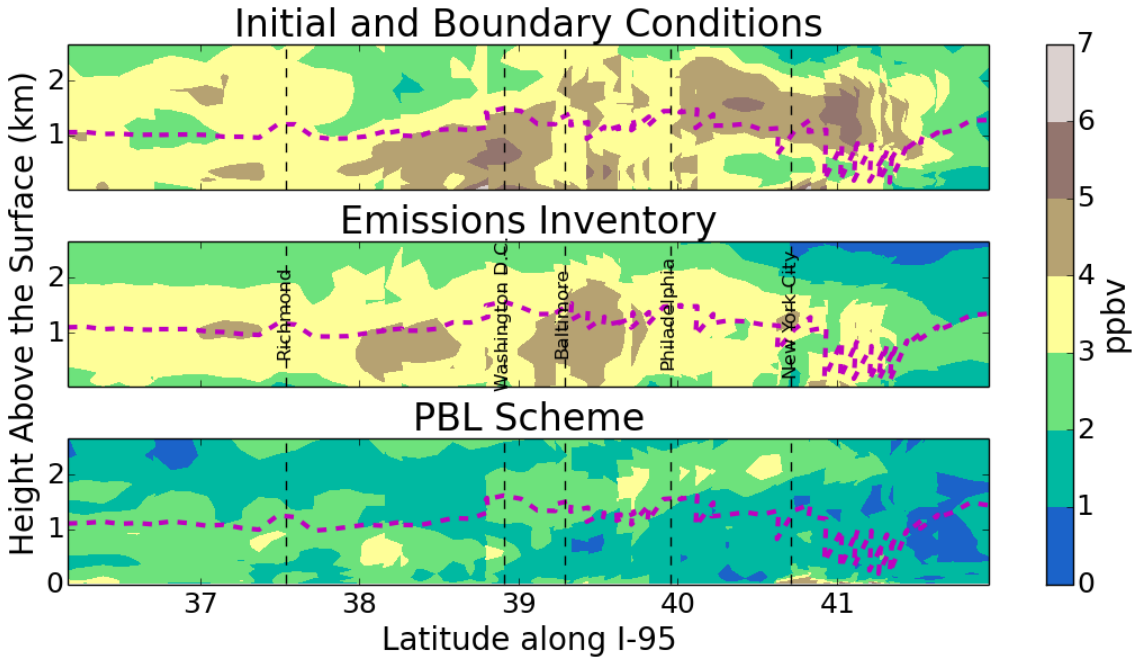

Figure 7: Temporal average of the cross-section of the sensitivity of MD8-O_3 during the upper-quintile.

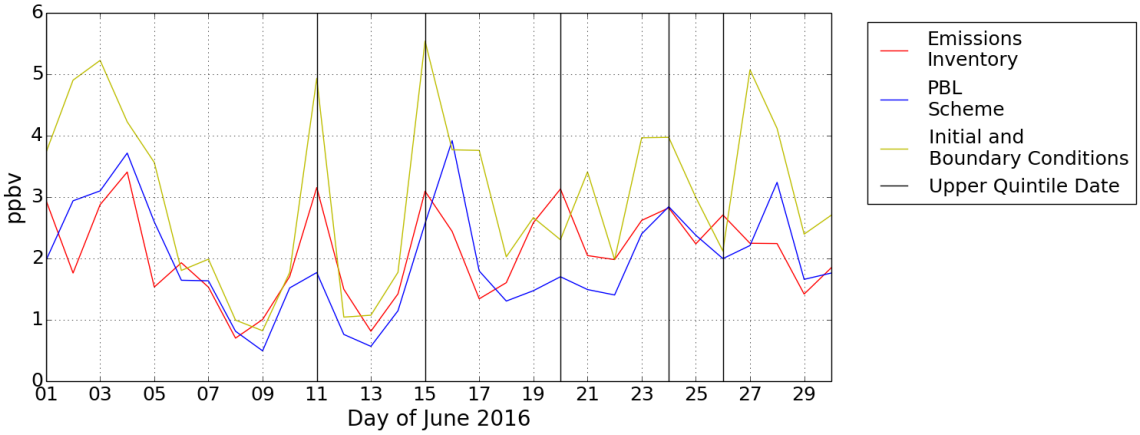

Figure 8: Spatially averaged timeseries of standard deviation of MD8-O_3 over land.

Table 3: Mean absolute error of the upper-quintile in the Analysis Region for each ensemble member.

Ensemble Member	Mean Absolute Error
CNTL	10.22
NEI-05	13.41
NEI-14*	9.11
MYJ	9.65
ACM2	10.34
ERA-GFS	11.70
MERRA-2	11.22

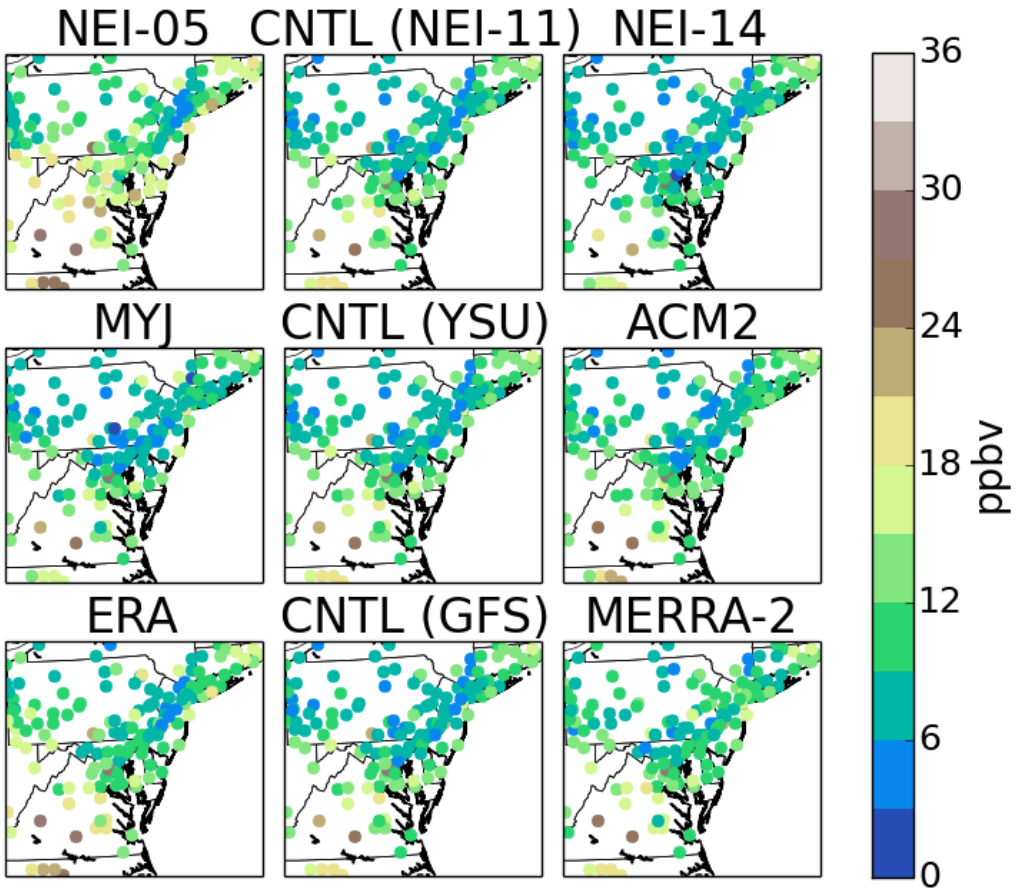

Figure 9: Mean absolute error of MD8-O_3 during the upper-quintile.

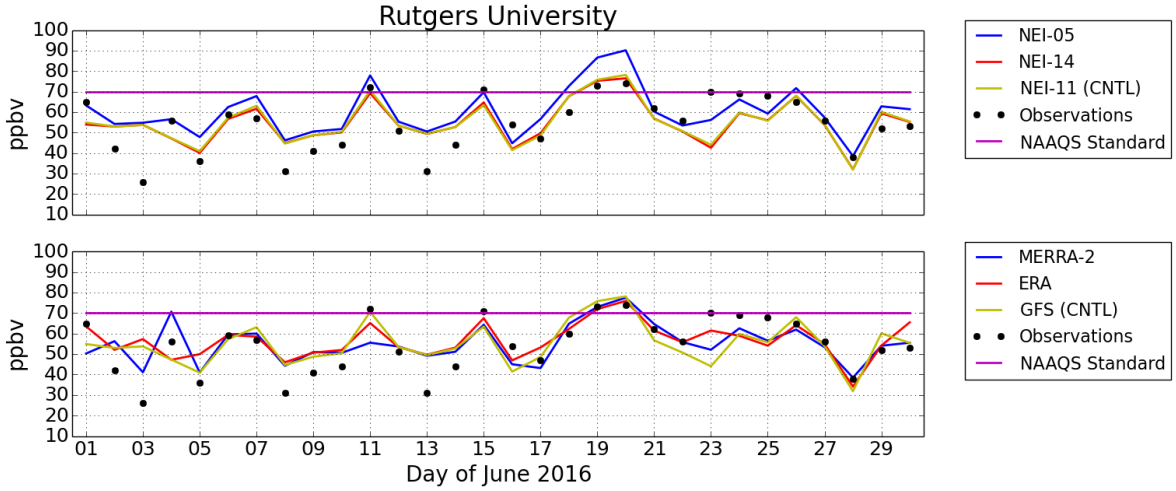

Figure 10: Timeseries of MD8-O_3 for the emissions inventory and initial and boundary conditions sub-ensembles at Rutgers University.

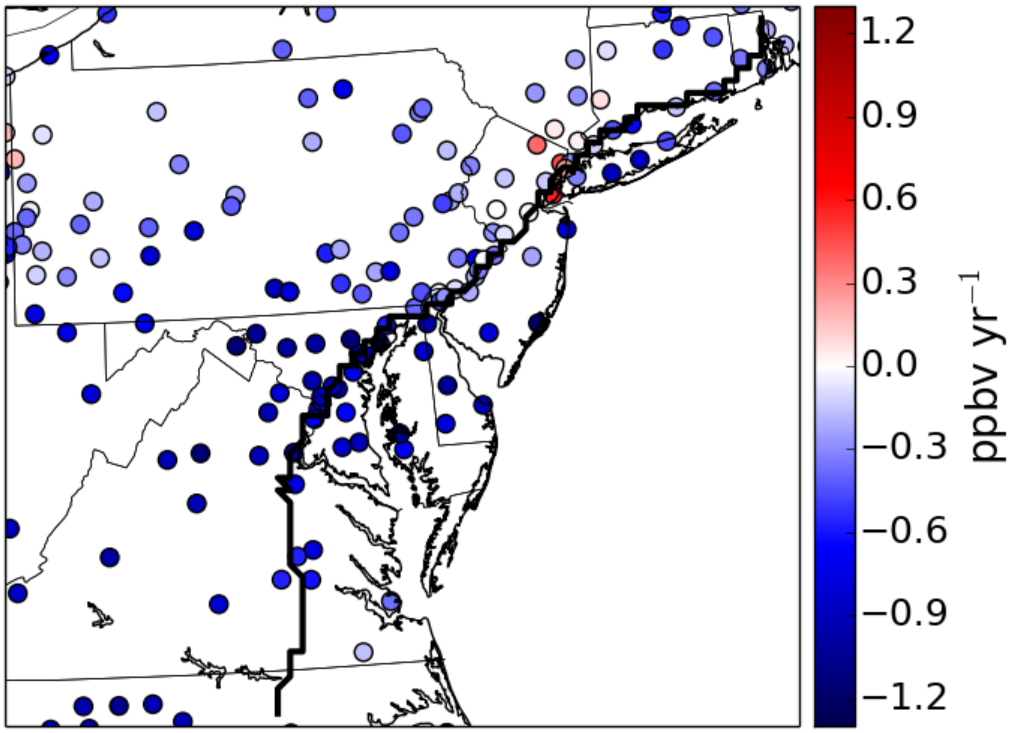

Figure 11: Average change of the mean absolute error of MD8-O_3 per emissions inventory year during the upper-quintile.

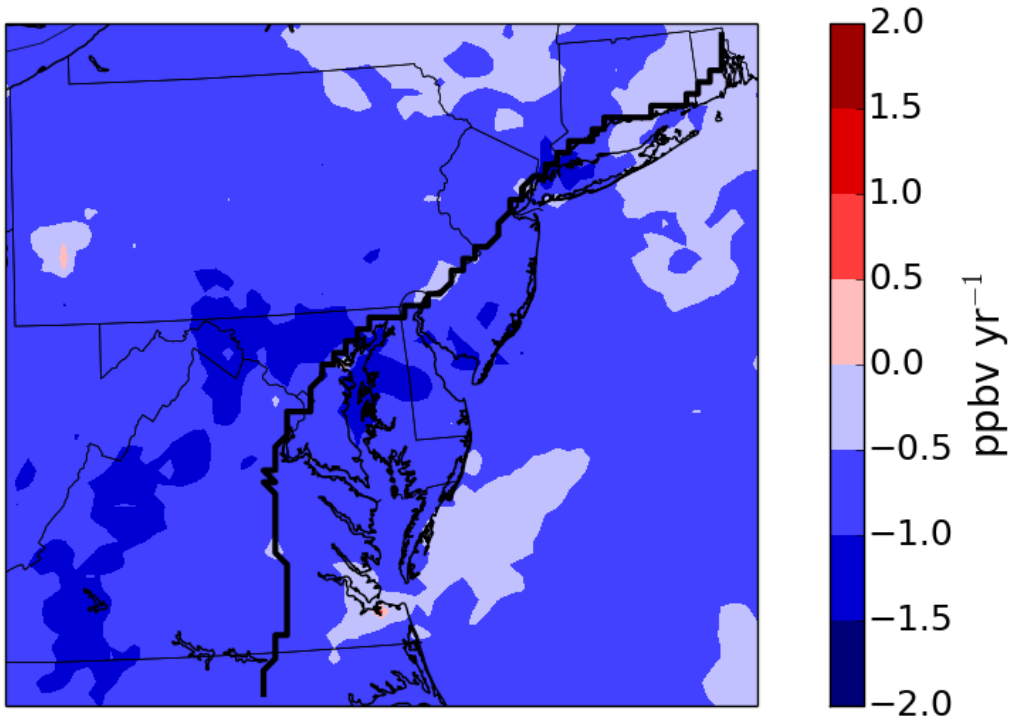

Figure 12: Average change of MD8-O_3 during the upper-quintile.

References

Anderson, D.C and Coauthors, 2014. Measured and modeled CO and NOy in DISCOVER-AQ: An evaluation of emissions and chemistry over the eastern US. *Atmos. Environ.*, **96**, 78-87, https://doi.org/10.1016/j.atmosenv.2014.07.004.

Azevedo, J.M., F.L. Gonçalves, and M. de Fátima Andrade, 2011: Long-range ozone transport and its impact on respiratory and cardiovascular health in the north of Portugal. *Int. J. Biometeorol.*, **55**, 187-202, doi:10.1007/s00484-010-0324-2.

Beekmann, M. and C. Derognat, 2003: Monte Carlo uncertainty analysis of a regional-scale transport chemistry model constrained by measurements from the atmospheric pollution over the Paris area (ESQUIF) campaign. *J. Geophys. Res.: Atmos.* **108**(D17), doi:10.1029/2003JD003391.

Bei, N., W. Lei, M. Zavala, and L.T. Molina, 2010: Ozone predictabilities due to meteorological uncertainties in the Mexico City basin using ensemble forecasts. *Atmos. Chem. Phys.*, **10**(13), 6295-6309, doi:10.5194/acp-10-6295-2010.

Bell, M.L., A. McDermott, S.L. Zeger, J.M. Samet, and F. Dominici, 2004: Ozone and short-term mortality in 95 US urban communities, 1987-2000. *JAMA*, **292**(19), 2372-2378, doi:10.1001/jama.292.19.2372.

Bell, M. and H. Ellis, 2004: Sensitivity analysis of tropospheric ozone to modified biogenic emissions for the Mid-Atlantic region. *Atmos. Environ.*, **38**(13), 1879-1889, doi:10.1016/j.atmosenv.2004.01.012.

Berge, E., H.C. Huang, J. Chang and T.H. Liu, 2001: A study of the importance of initial conditions for photochemical oxidant modeling. *J. Geophys. Res.: Atmos.*, **106**(D1), 1347-1363, doi:10.1029/2000JD900227.

Borge, R., V. Alexandrov, J.J. Del Vas, J. Lumbreras, and E. Rodríguez, 2008: A

comprehensive sensitivity analysis of the WRF model for air quality applications over the Iberian Peninsula. *Atmos. Environ.*, **42**(37), 8560-8574, doi:10.1016/j.atmosenv.2008.08.032.

Byun, D., J. Young, G. Gipson, J. Godowitch and F. Binkowski, 1997: Description of the Models-3 Community Multiscale Air Quality(CMAQ) Modeling System.

Castellanos, P., J.W. Stehr, J.R. Dickerson, and S.H. Ehrman, 2009: The sensitivity of modeled ozone to the temporal distribution of point, area, and mobile source emissions in the eastern United States. *Atmos. Environ.*, **43**(30), 4603-4611, doi:10.1016/j.atmosenv.2009.05.045.

Cheng, F.Y., Chin, S.C. and Liu, T.H., 2012. The role of boundary layer schemes in meteorological and air quality simulations of the Taiwan area. *Atmos. Environ.*, **54**, 714-727, doi:10.1016/j.atmosenv.2012.01.029.

Cuchiara, G.C., X. Li, J. Carvalho, and B. Rappenglück, 2014: Intercomparison of planetary boundary layer parameterization and its impacts on surface ozone concentration in the WRF/Chem model for a case study in Houston/Texas. *Atmos. Environ.*, 96, 175-185, doi:10.1016/j.atmosenv.2014.07.013.

Davidson, P., K. Schere, R. Draxler, S. Kondragunta, R.A. Wayland, J.F. Meagher, and R. Mathur, 2008: Toward a US national air quality forecast capability: Current and planned capabilities. *Air Pollution Modeling and Its Application XIX*, Springer, Dordrecht. 226-234.

Dee, D.P. and Coauthors, 2011: The ERA-Interim reanalysis: Configuration and performance of the data assimilation system. *Q. J. R. Meteorol. Soc.*, **137**(656), 553-597, doi:10.1002/qj.828.

Dudhia, J., 1989. Numerical study of convection observed during the winter monsoon

experiment using a mesoscale two-dimensional model. *J. Atmos. Sci.*, **46**(20), 3077-3107, doi:10.1175/1520-0469(1989)046%3C3077:NSOCOD%3E2.0.CO;2.

EPA, 2015. 2011 National emissions inventory, version 2, Technical support document, Office of Air and Radiation. [Available online at: https://www.epa.gov/air-emissions-inventories/2011-national-emissions-inventory-nei-documentation]

Fiore, A.M., L.W Horowitz, D.W. Purves, H. Levy, M.J. Evans, Y. Wang, Q. Li and R.M. Yantosca, 2005: Evaluating the contribution of changes in isoprene emissions to surface ozone trends over the eastern United States. *J. Geophys. Res.: Atmos.*, **110**(D12). doi: 10.1029/2004JD005485

Frost, G.J., and Coauthors, 2006: Effects of changing power plant NOx emissions on ozone in the eastern United States: Proof of concept. *J. Geophys. Res.: Atmos.*, **111**(D12). doi:10.1029/2005JD006354.

Gelaro, R., and Coauthors, 2017: The Modern-Era Retrospective Analysis for Research and Applications, Version 2 (MERRA-2). *J. Clim.* **30**, 5419–5454, doi:10.1175/JCLI-D-16-0758.1.

Gent, J.F., E.W. Triche, T.R. Holford, K. Belanger, M.B. Bracken, W.S. Beckett and B.P. Leaderer, 2003: Association of low-level ozone and fine particles with respiratory symptoms in children with asthma. *JAMA*, **290**(14), 1859-1867, doi:10.1001/jama.290.14.1859.

Gilliam, R.C., C. Hogrefe, J.M. Godowitch, S. Napelenok, R. Mathur and S.T. Rao, 2015. Impact of inherent meteorology uncertainty on air quality model predictions. *J. Geophys. Res.: Atmos.* **120**(23), 12259-12280, doi:10.1002/2015JD023674.

Grell, G.A. and D. Dévényi, 2002: A generalized approach to parameterizing convection

combining ensemble and data assimilation techniques. *Geophys. Res. Lett.*, **29**(14). doi:10.1029/2002GL015311.

Grell, G.A., S.E. Peckham, R. Schmitz, S.A. McKeen, G. Frost, W.C. Skamarock and B. Eder, 2005: Fully coupled "online" chemistry within the WRF model. *Atmos. Environ.*, **39**(37), 6957-6975, https://doi.org/10.1016/j.atmosenv.2005.04.027.

Guenther, C.C., 2006. Estimates of global terrestrial isoprene emissions using MEGAN (Model of Emissions of Gases and Aerosols from Nature). *Atmos. Chem. Phys.* **6**, 3181-3210, https://doi.org/10.5194/acp-6-3181-2006.

Hariprasad, K.B.R.R., C.V. Srinivas, A.B. Singh, S.V.B. Rao, R. Baskaran and B. Venkatraman, 2014: Numerical simulation and intercomparison of boundary layer structure with different PBL schemes in WRF using experimental observations at a tropical site. *Atmos. Res.*, **145**, 27-44, https://doi.org/10.1016/j.atmosres.2014.03.023.

Hodnebrog, Ø., F. Stordal and T.K. Berntsen, 2011: Does the resolution of megacity emissions impact large scale ozone? *Atmos. Environ.*, **45**(38), 6852-6862, https://doi.org/10.1016/j.atmosenv.2011.01.012.

Hong, S.Y. and J.O.J. Lim, 2006: The WRF single-moment 6-class microphysics scheme (WSM6). *J. Korean Meteor. Soc*, **42**(2), 129-151.

Hong, S.Y., Y. Noh and J. Dudhia, 2006: A new vertical diffusion package with an explicit treatment of entrainment processes. *Mon. Weather Rev.*, **134**(9), 2318-2341, https://doi.org/10.1175/MWR3199.1.

Hu, X.M., D.C. Doughty, K.J. Sanchez, E. Joseph, and J.D. Fuentes, 2012: Ozone variability in the atmospheric boundary layer in Maryland and its implications for vertical transport model. *Atmos. Environ.*, **46**, 354-364, https://doi.org/10.1016/j.atmosenv.2011.09.054.

Jiménez, P.A., J. Dudhia, J.F. González-Rouco, J. Navarro, J.P. Montávez and E. García-

Bustamante, 2012: A revised scheme for the WRF surface layer formulation. *Mon. Weather Rev.*, **140**(3), 898-918, https://doi.org/10.1175/MWR-D-11-00056.1.

Jiménez, P., R. Parra and J.M. Baldasano, 2007: Influence of initial and boundary conditions for ozone modeling in very complex terrains: A case study in the northeastern Iberian Peninsula. *Env. Model. Soft.*, **22**(9), 1294-1306, https://doi.org/10.1016/j.envsoft.2006.08.004.

Kim, S.W., Heckel, A., McKeen, S.A., Frost, G.J., Hsie, E.Y., Trainer, M.K., Richter, A., Burrows, J.P., Peckham, S.E. and Grell, G.A., 2006. Satellite-observed US power plant NOx emission reductions and their impact on air quality. *Geophys. Res. Lett.*, **33**(22).

Lorenz, E.N., 1963. Deterministic nonperiodic flow. *J. Atmos. Sci.*, **20**(2), 130-141, https://doi.org/10.1175/1520-0469(1963)020<0130:DNF>2.0.CO;2.

Lorenz, E.N., 1969. Atmospheric predictability as revealed by naturally occurring analogues. *J. Atmos. Sci.*, **26**, 636-646

Madronich, S., 1987. Photodissociation in the atmosphere: 1. Actinic flux and the effects of ground reflections and clouds. *J. Geophys. Res.: Atmos.*, **92**(D8), 9740-9752, doi:10.1029/JD092iD08p09740.

Mallet, V. and B. Sportisse, 2006. Uncertainty in a chemistry-transport model due to physical parameterizations and numerical approximations: An ensemble approach applied to ozone modeling. *J. Geophys. Res.: Atmos.*, **111**(D1), doi:10.1029/2005JD006149.

Mena-Carrasco, M. and Coauthors, 2009: Assessing the regional impacts of Mexico City emissions on air quality and chemistry. *Atmos. Chem. Phys.*, **9**(11), 3731-3743, https://doi.org/10.5194/acp-9-3731-2009.

Melhauser, C. and F. Zhang, 2012. Practical and intrinsic predictability of severe and convective weather at the mesoscales. *J. Atmos. Sci.*, **69**(11), 3350-3371, https://doi.org/10.1175/JAS-D-11-0315.1.

Misenis, C. and Y. Zhang, 2010. An examination of sensitivity of WRF/Chem predictions to physical parameterizations, horizontal grid spacing, and nesting options. *Atmos. Res.*, **97**(3), 315-334, https://doi.org/10.1016/j.atmosres.2010.04.005.

Mlawer, E.J., S.J. Taubman, P.D. Brown, M.J. Iacono and S.A. Clough, 1997. Radiative transfer for inhomogeneous atmospheres: RRTM, a validated correlated-k model for the longwave. *J. Geophys. Res.: Atmos.*, **102**(D14), 16663-16682, doi:10.1029/97JD00237.

Monin, A.S. and A.M.F. Obukhov, 1954: Basic laws of turbulent mixing in the surface layer of the atmosphere. *Contrib. Geophys. Inst. Acad. Sci. USSR*, **151**(163), 187.

Otte, T.L. and Coauthors, 2005. Linking the Eta model with the Community Multiscale Air Quality (CMAQ) modeling system to build a national air quality forecasting system. *Wea. Forecasting*, **20**(3), 367-384.

Pan, L., D. Tong, P. Lee, H.C. Kim and T. Chai, 2014: Assessment of NOx and O3 forecasting performances in the US National Air Quality Forecasting Capability before and after the 2012 major emissions updates. *Atmos. Environ.*, **95**, 610-619, https://doi.org/10.1016/j.atmosenv.2014.06.020.

Pleim, J.E., 2011: Comment on "Simulation of surface ozone pollution in the central Gulf coast region using WRF/Chem model: sensitivity to PBL and land surface physics". *Adv. Meteorolo*, http://dx.doi.org/10.1155/2011/464753.

Ryan, W.F., 2016: The air quality forecast rote: Recent changes and future challenges. *J. Air Waste Manage. Assoc.*, **66**(6), 576-596. doi: 10.1080/10962247.2016.1151469

Ryan, W.F., and Coauthors, 1998: Pollutant transport during a regional O3 episode in the mid-Atlantic states. *J. Air Waste Manage. Assoc.*, **48**(9), 786-797. doi: 10.1080/10473289.1998.10463737

Seaman, N.L., 2000: Meteorological modeling for air-quality assessments. *Atmos.*

Environ., **34**(12), 2231-2259, https://doi.org/10.1016/S1352-2310(99)00466-5.

Seaman, N.L. and S.A. Michelson, 2000: Mesoscale meteorological structure of a high-ozone episode during the 1995 NARSTO-Northeast study. *J. Appl. Meteorol.*, **39**(3), 384-398.

Skamarock, W.C., J.B. Klemp, J. Dudhia, D.O. Gill, D.M. Barker, W. Wang and J.G. Powers, 2005: A description of the advanced research WRF version 2 (No. NCAR/TN-468+ STR). National Center For Atmospheric Research Boulder Co Mesoscale and Microscale Meteorology Div.

Stauffer, R.M., and Coauthors, 2015: Bay breeze influence on surface ozone at Edgewood, MD during July 2011. *J. Atmos. Chem.*, **72**(3-4), 335-353. DOI 10.1007/s10874-012-9241-6.

Stockwell, W.R., F. Kirchner, M. Kuhn and S. Seefeld, 1997: A new mechanism for regional atmospheric chemistry modeling. *J. Geophys. Res.: Atmos.*, **102**(D22), 25847-25879, doi:10.1029/97JD00849.

Tewari, M. and Coauthors, 2004: Implementation and verification of the unified NOAH land surface model in the WRF model. In *20th Conference on weather analysis and forecasting/16th conference on numerical weather prediction* (Vol. 1115). [Available online at https://ams.confex.com/ams/84Annual/techprogram/paper_69061.htm]

Tie, X., G. Brasseur and Z. Ying, 2010: Impact of model resolution on chemical ozone formation in Mexico City: application of the WRF-Chem model. *Atmos. Chem. Phys.*, **10**(18), 8983-8995, doi:10.5194/acp-10-8983-2010.

Tong, D., and Coauthors, 2016: Impact of the 2008 Global Recession on air quality over the United States: Implications for surface ozone levels from changes in NOx emissions. *Geophys. Res. Lett.*, **43**(17), 9280-9288, doi:10.1002/2016GL069885.

Tong, D.Q., and Coauthors, 2015: Long-term NO x trends over large cities in the United States

during the great recession: Comparison of satellite retrievals, ground observations, and emission inventories. *Atmos. Environ.*, **107**, 70-84, https://doi.org/10.1016/j.atmosenv.2015.01.035.

Travis, K.R., and Coauthors, 2016: Why do models overestimate surface ozone in the Southeast United States? *Atmos. Chem. Phys.*, **16**(21), 13561-13577, https://doi.org/10.5194/acp-16-13561-2016.

Vijayaraghavan, K., C. Lindhjem, A. DenBleyker, U. Nopmongcol, J. Grant, E. Tai and G. Yarwood, 2012: Effects of light duty gasoline vehicle emission standards in the United States on ozone and particulate matter. *Atmos. Environ.*, **60**, 109-120, https://doi.org/10.1016/j.atmosenv.2012.05.049.

Yerramilli, A., and Coauthors 2010: Simulation of surface ozone pollution in the central gulf coast region using WRF/Chem Model: Sensitivity to PBL and Land Surface Physics. *Adv. Met.*, 2010, https://doi.org/10.5094/APR.2012.005.

Zhang, F., A. Odins, and J. W. Nielsen-Gammon, 2006: Mesoscale predictability of an extreme warm-season rainfall event. *Wea.Forecasting*, **21**,149–166.

Zhang, F., N. Bei, J.W. Nielsen-Gammon, G. Li, R. Zhang, A. Stuart and A. Aksoy, 2007: Impacts of meteorological uncertainties on ozone pollution predictability estimated through meteorological and photochemical ensemble forecasts. *J. Geophys. Res.: Atmos.*, **112**(D4), doi:10.1029/2006JD00

Zhong, M. and Coauthors 2016: Air quality modeling with WRF-Chem v3.5 in East Asia: sensitivity to emissions and evaluation of simulated air quality. *Atmos. Chem. Phys.* , **9**(3), 1201-1218, doi:10.5194/gmd-9-1201-2016.